INTERNATIONAL SOCIETY FOR SOIL MECHANICS AND GEOTECHNICAL ENGINEERING

SIMSG   ISSMGE

XVII European Conference

ECSMGE 2019
Reykjavik

on Soil Mechanics
and Geotechnical Engineering

On distributed strains in a CFA pile via DFOSs measurements and numerical analysis

Déformations distribuées dans un pieu en CFA obtenues par des mesures de DFOS et analyse numérique

S. Cola, S. Bersan, E. Michielin, F. Tchamaleu Pangop, P. Simonini
Department of Civil, Environmental and Architectural Engineering, University of Padova, Italy

L. Schenato
National Research Council, Research Institute for Geo-Hydrological Protection, Padova, Italy

L. Palmieri
Department of Information Engineering, University of Padova, Italy

O. Bergamo
Veneto Strade s.p.a., Italy

ABSTRACT: Fibre Optic Sensors (FOSs) offer unprecedented possibilities for the monitoring of engineering structures, such as foundation systems. Notably, the type of FOSs known as Distributed Fibre Optic Sensors (DFOSs) has the capability of monitoring variations in the observed physical field, such as strain and temperature, with spatial continuity along the fibre. This paper presents and discusses the distributed strain measurements collected along a continuous flight auger (CFA) pile, belonging to the foundation raft of a new bridge subjected to an acceptance static load test. The monitoring was performed using a DFOS system, which works according to the optical frequency domain reflectometry (OFDR) method and provides a spatial resolution of 10 mm and a strain resolution of 1 με. The in-situ monitoring results were used to calibrate a 3D Finite Element Model of the foundation system. The soil properties for the numerical model were also selected on the basis of a load test previously carried out on a similar pile at the same site.

RÉSUMÉ: Les capteurs à fibre optique (FOS) offrent des possibilités sans précédent pour le contrôle des structures d'ingénierie, telles que les systèmes de fondations. Spécialement, le type de FOS connu sous le nom de capteur à fibres optiques distribuées (DFOS) a la capacité de surveiller les variations du champ physique observé, telles que la déformation et la température, avec continuité spatiale le long de la fibre. Cet article présente et discute des mesures de déformation distribuées collectées le long d'un pieu à la tarière à vis continu (CFA), appartenant au radier de fondation d'un nouveau pont soumis à un test de réception en condition statique. Le contrôle a été effectuée à l'aide d'un système DFOS fonctionnant selon la méthode de réflectométrie optique du domaine de fréquence (OFDR) et offrant une résolution spatiale de 10 mm et une résolution de déformation de 1 με. Les résultats du contrôle in situ ont été utilisés pour calibrer un modèle 3D d'éléments finis du système de fondation. Les propriétés du sol utilisé dans le modèle ont également été sélectionnées à la lumière d'un test de charge précédemment effectué sur un pieu similaire sur le même site.

Keywords: Raft foundation, CFA piles, Distributed Fibre optic sensors, Optical frequency domain reflectometer, Numerical model.

1 INTRODUCTION

Recent research and development in the field of structural health monitoring for engineering applications are aimed to improve the resilience of structural systems to both repetitive serviceability loads and ultimate limit conditions and, at the same time, to permit a prompt recognition of the critical behaviour of a system (Brownjohn, 2007) to set up a more efficient condition-based maintenance.

As civil and geotechnical works concerns, the strain and/or stress state can be determined with the use of Distributed Fibre Optic Sensors (DFOSs). These sensors, based on the Fibre Optic technology, allow the direct measure of strain and/or temperature in a large number of positions for long-range sensing. By proper transducing mechanisms, it is possible to convert the measured strain and temperature into other suitable physical quantities, and therefore use the DFOSs as a distributed load cells, pressure transducers, etc.

The use of DFOSs has sharply increased in the last 30 years because they offer many advantages respect the traditional sensors based on spot measurement of monitored quantities. The DFOS are easy to install, not affected by aggressive substances or by the electromagnetic interference and economically convenient for application requiring a high number of measurement points. By integrating DFOSs to the civil structures, the designer knows in real time the working condition along with the whole life of the structure (Soga, 2014).

This paper presents the application of DFOSs to evaluate the behaviour of a continuous flight auger (CFA) pile, belonging to the foundation raft of a new bridge, during the acceptance load test carried out on the bridge. This study is the extension of a previous study performed on a similar pile realized in the same site and subjected to a design load test (Bersan et al., 2018).

2 OPERATING PRINCIPLES OF DFOSs

The operating principle of Distributed Optical Fibre Sensors is based on the injection of a light wave in an optical fibre and on the analysis of the back reflected light signal generated by the scattering effects in the silica composing the fibre. DFOSs currently available exploit one or more of the three different scattering phenomena that take place in the fibre, namely the Brillouin, Rayleigh, and Raman scattering (Schenato, 2017). The Brillouin-based DFOSs are the most used for the measurement of strain over long range and many applications of these sensors in geotechnical engineering have been carried out in the recent past (e.g., De Battista et al., 2016). The applications based on Rayleigh back-scattering are less common, mostly due to the limited range. Nonetheless, since they permit to obtain very high-resolution data of strain and/or temperature, they are often used in small scale physical models and set-ups, or in limited area, where dense spatial sampling is required (Bersan et al., 2018; Schenato et. al, 2017).

Among the optical sensing technique exploiting the Rayleigh scattering, the Optical Frequency Domain Reflectometry (OFDR) assures a spatial resolution of some millimetres (Palmieri and Schenato, 2013), while Brillouin-based sensors usually are limited to some tens of centimetres. (Schenato, 2017).

In the present study, five optical fibre cables embedded in the pile are used and interrogated by a commercial OBR4600 for the measurement of strain and temperature.

It is important to note that several studies have been already carried out on CFA pile instrumented with DFOSs and subjected to static load tests (e.g. Kania and Sorensen, 2018). The authors are not aware of published applications of DFOSs for the monitoring of at long term behaviour of piles in serviceability state. As the effects of strain and temperature are coupled in the fibre response, to retrieve only one parameter, the other has to be considered constant or measured with another sensor. Therefore, in the present

study particular care was put in determining the mechanical strain from measurements acquired in different time with changing temperature field.

3 CASE STUDY CHARACTERISTICS

The here considered bridge was realized in 2016-2017 as a part of a new road named "Terraglio Est" in Veneto region (Italy). The bridge bearing structure is a steel tied arch bridge, with a span 65m long and 18.80m wide (Figure 1). Two concrete rafts, founded on 20 and 22 Continuous Fly Auger (CFA) piles, support the North and South abutments, respectively. In the North abutment, the piles are 24m long and 60 cm in diameter; their head is at +6.6m above sea level (a.s.l.). The foundation raft of the North abutment is 19.20m long, 5.50m wide and 1.5m thick (Figure 2a). The load is transferred to each

abutment by 2 seismic supports, each of them located on a square concrete slab.

Steel bars of 24mm-diameter and 12m long compose the longitudinal reinforcing system of the piles: 12 bars are in the upper portion, 6 in the lower portion, with an overlapping of 1.2m. The 12mm spiral reinforcement is characterized by an interspace of 15cm in the first upper 5m and of 20cm in the remaining portion.

The automatic software recording the machine parameters during pile construction indicated a relatively constant pile diameter equal to 60cm along the shaft, with an enlargement of almost 1m in the deepest section of 1 m.

Cone Penetration Test, Standard Penetration Test and borehole tests were carried out in order to identify the soil profile and properties. The soil profile is depicted in Figure 3.
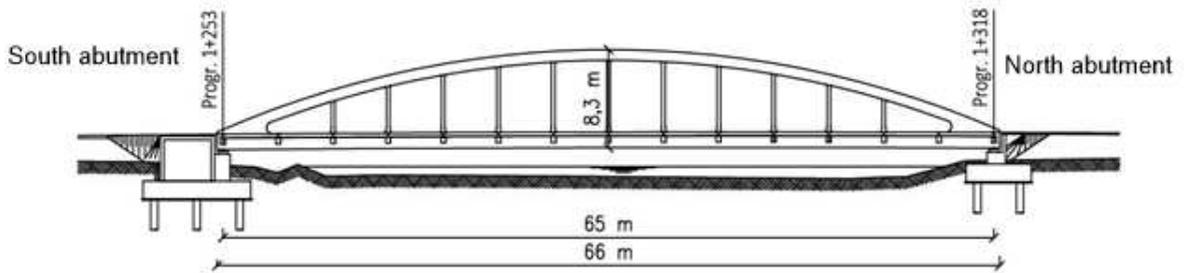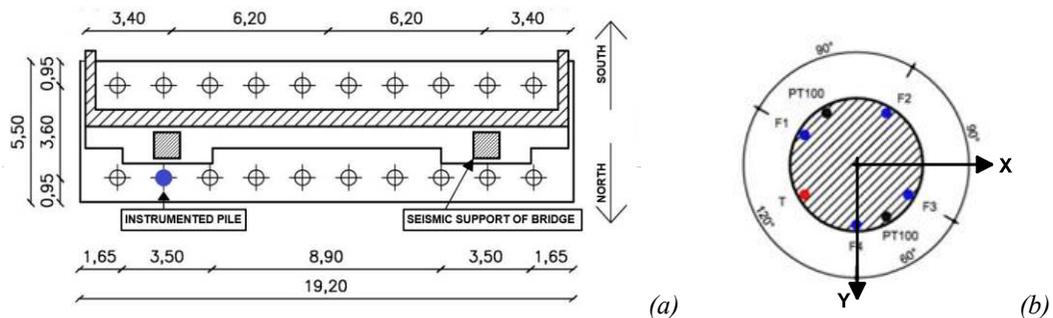

Figure 1. Longitudinal section of the bridge.

Figure 2. Plant of the North abutment (a) and transversal section of the instrumented CFA pile (b).

3.1 Measuring system on the tested pile

One of the piles belonging to the North abutment (blue coloured in the Figure 2*a*) was instrumented with DFOSs in order to study the pile strain distribution during the construction phases and the subsequent acceptance load test performed on the bridge. Five lengths of fibre optic cables were installed in the tested pile: 4 were BRUsens V9 strain cables (F1, F2, F3 e F4 in Figure 2*b*), especially design for strain measurement; the 5th cable was a BRUsens temperature cable 85° (T in Figure 2*b*), working in free strain condition is used to measure only thermal strain. The 5th cable was utilized because, in the case of long term monitoring, temperature variation of the external environment could produce strain equivalent variations which are not negligible even at larger depth, affecting the estimate of the strain in following loading phases. In addition to DFOSs, some Resistance Temperature Detectors (RDT) (PT100 in Figure 2*b*) were set up along the pile at +5.0, +4.1, +2.6, +1.1, -0.4, -3.4 and -6.4m a.s.l. Their use is of paramount importance in the study, because they give optimal precision, high stability and durability.

All the strain distributed optical fibre cables were pre-strained to about 3200με applying a dead weight of 150 N in order to ensure the presence of tension conditions in the cables. Since the maximum elastic tension for this cable is 260N with an elastic strain range of 1%, the pre-strain was kept inside the elastic range. The cables were also fixed to the longitudinal bars with 2m spaced plastic ties.

The DFOS was interrogated with the OFDR technique, which, in this case, ensured a spatial resolution of 10 mm. If the geometrical and mechanical characteristics of the pile are known, from the measured strains it is possible to determine the longitudinal profile of axial stress and the bending moment along the pile.

Note that, in an area close the South abutment another pile, with the same characteristics and equipped with the same DFOSs system, was previously realized and subjected to a design load test (Bersan et al., 2018). In that case, the maximum bearing capacity resulted about 3000 kN, i.e. about 2.5 time the calculated serviceability load. The maximum compression strains recorded at the pile head at maximum load were about 200-350 με, with a relatively linear strain distribution along the pile according to a gradual load transfer along the lateral pile surface.

In the present study, the optical fibres were interrogated in the following phases:
a) At the end of construction of the North abutment on 21.10.2016. This was the first reading, and therefore it becomes the reference reading for all the subsequent measurements;
b) After setting up the bridge steel structure, on 30.01.2017;
c) After the bridge completion (08.03.2017), with the setup of the *predalles* plates, concrete platform and earth embankment for the access ramp (started in February 2017);
d) Before the acceptance load test on 10.05.2017;
e) During the acceptance load test with a load equal to 1200kN located in the middle of the span (10.05.2017);
f) During the acceptance load test with a load equal to 2400kN located in the middle of the span (10.05.2017);
g) At the end of unloading phase.

As for the optical cables, the PT100 returned the variation of temperature from the reference reading that is in date 21.10.2016.

4 STRAIN AND TEMPERATURE DATA

Figure 3 reports the vertical profiles of the vertical strains $με_{meas}$ recorded by the optical cables at the steps (*b*) and (*d*), i.e. after the place of the steel structure and before the acceptance test. Moreover, the vertical distribution of temperature variations registered by T cable and PT100s at steps (*b*) and (*d*) are also reported in Figure 3.

Due to the pile position, it is possible to suppose that in step (*b*) the pile was subjected to an axial load with a very small bending moment. This hypothesis is confirmed by FEM calculations (see section 5) but also by the $\mu\varepsilon_{meas}$ profiles, which exhibit very small relative differences. Otherwise, in step (*d*), the differences in $\mu\varepsilon_{meas}$ in the portion between +5 and -3 m a.s.l. indicate a deflection of the upper part of the pile and consequently the occurrence of bending moments. In fact, near the pile head the $\mu\varepsilon_{meas}$ of F1 and F2 are greater than those of F3 and F4. On the contrary, below +3.5m a.s.l. there is an inversion of the bending moment, since $\mu\varepsilon_{meas}$ in F1

and F2 becomes smaller than those in F3 and F4.

Figure 3 also shows two unexpected responses compared to the behaviour observed in the static load test (Bersan et al., 2018). The first one is a very high compression strain (about -250$\mu\varepsilon$) at the pile head in step (*b*). This high strain is comparable with the maximum compression strain reached in the design load test at the maximum load of about 3000 kN (Bersan et al., 2018), but it rapidly reduces in the first 5 m of the pile (e.g., $\mu\varepsilon_{meas} \approx 25\ \mu\varepsilon$ at +0m a.s.l.). This high compression strain cannot be a consequence of the loads applied through the slab to the piles, that should stay below 150 kN; it could be due to concrete shrinkage caused by a decrease of the
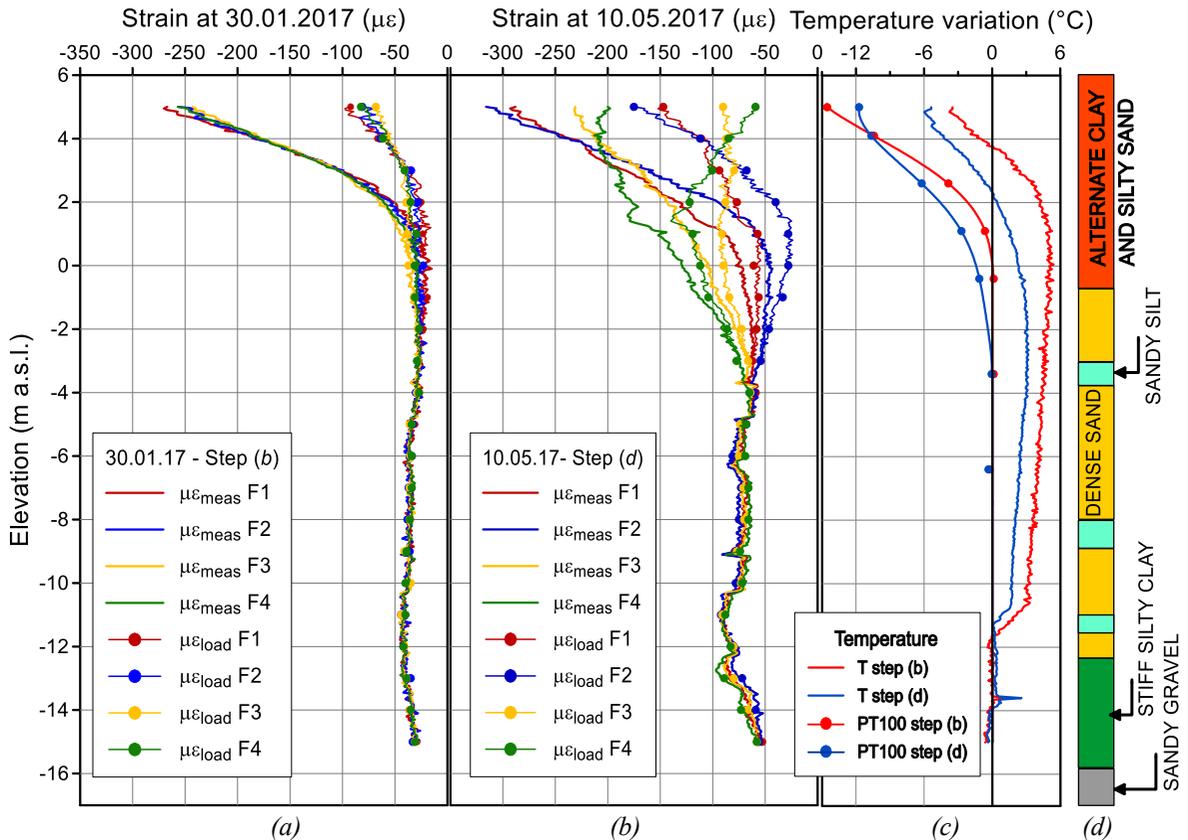

Figure 3. Vertical strains $\mu\varepsilon_{meas}$ recorded by the DFOSs on (a) 30.01.2017 and (b) 10.05.2017 and their comparison with net strains $\mu\varepsilon_{load}$ obtained after the correction; (c) Temperature variation measured by T cable and PT100 sensors; (d) Reconstructed soil stratigraphy.

environmental temperature or to creep occurred after the reference reading.

The second unexpected behaviour is the increase of compression strain in the deepest part of the pile, i.e. between +0m and -12m a.s.l.: this may be justified by the reduction of the number of the reinforcement bars or by the occurrence of a negative skin friction, as a consequence of the compression of soft soil just below the slab.

Finally, it is interesting to observe how the optical measures are able to show the presence of thin layers of soft soil: e.g. $\mu\varepsilon_{meas}$ presents a local increase at -9m a.s.l. according to lower q_c in CPT profile.

It is interesting to compare temperature profiles inferred either by optical cables and by temperature sensors PT100 (Figure 3c).

According to PT100 data, the temperature variation only affects the upper 6 m of the pile and shows no variation up to larger depths. These trends are in accordance with observation of Cunat et al. (2012) in winter-spring period.

On the contrary fibre temperature profile, are characterized by unreasonable positive variation from +4m to -12 m that cannot be justified by natural temperature gradient. Moreover, an abrupt variation of temperature at –12 m is observed. This unexpected trend may likely be due to the presence of some constraints given by the ties fixing the cable to the reinforcing bars, resulting in an almost constant positive strain exerted to the fiber down to that point and a corresponding equivalent right-shift of the temperature profile.

For future monitoring with temperature cables, it would be very important find out another method of installation in order to ensure correct measurements.

In order to get the real mechanical strains due to axial and bending stresses occurring in the pile (named $\mu\varepsilon_{load}$ in the following), it is straight forward to remove from total strains $\mu\varepsilon_{meas}$ the thermal ones, i.e. the concrete compression strains due to the temperature reduction (named concrete thermal strain in the following). To calculate the thermal contraction, the temperature variation at PT100s was multiplied by the cubic thermal expansion coefficient of concrete, assumed equal to $C_{con}=1.2\cdot10^{-5}$ °C^{-1}. Since DFOSs supplied a continuous strain profile, a distributed temperature profile was obtained by spline interpolation of PT100 measures (Figure 3). With this correction the compression strain $\mu\varepsilon_{load}$ induced at the pile head by the bridge construction results signficantly lower, i.e. less than 100$\mu\varepsilon$ and 180 $\mu\varepsilon$ at stages (b) and (d) respectively.

5 PILE AXIAL FORCES AND BENDING MOMENTS

The axial forces acting in the pile at every depth was then calculated from $\mu\varepsilon_{load}$, multiplying the average values by the pile elastic stiffness EA. To compute the bending moments with respect to the local axes X and Y indicated in Figure 2b (respectively parallel and normal to the largest side of the abutment), the data from optical fibres have been corrected accounting for their relative position to the centre of cross section of the pile.

6 NUMERICAL MODEL

In order to study the geotechnical behaviour of the North abutment and its foundation system, a preliminar 3D model was created with the MIDAS GTS NX finite element model. The analysed geometry is limited for symmetry to half abutment. The geotechnical soil profile considered for the simulation is summarized in table 1: the ground is schematised in four layers described with Mohr Coulomb elasto-plastic law, with properties estimated in this first attempt from CPT tests. The abutment and the piles are simulated uning a linear elastic material model, while the pile-ground contact is simulated with an elastic-plastic interface according to the Mohr-Coulomb friction law. In the model, all the

Table 1. Material properties simulated in the numerical analysis

Soil Material	Alternate clay and silty sand	Dense Sand	Stiff clay	Sandy gravel
Depth [m]	GL÷6.7	≥17.1	≥21.7	<21.7
γ_{sat} [kN/m³]	16	18.5	17	20
C' [kPa]	2	-	10	-
ϕ' [deg]	35	40	28	48
E [MPa]	6	100	20	120
ν' [-]	0.35	0.3	0.4	0.3

previously listed loading phases were simulated in order to determine, for each of them, the variation of the axial forces and bending moments of the piles, to be compared with those derived from the measurements with the optical fibres. The preliminary analysis provides only some qualitative results, and a more detailed calibration of the model is planned in the future.

Figures 4*a* and 4*b* report the vertical distribution of axial forces and bending moments with respect to the X-axis, comparing the trends for steps (*b*) and (*d*) obtained by in-situ measurements and by numerical simulation. Even if the experimental trends and the calculated ones present some similarities, it is evident that the axial forces obtained on the base of DFOSs strains at every depth are too much higher if compared with the values supplied by FE analysis, but also with the values predicted by the designers.

Considering the bending moments, the numerical and measured moments at step (*b*) are almost equal and quite negligible, as predicted by designers. On the contrary, at step (*d*) the bending

moments are significant: particularly, both the in-situ measurements and the FE analysis indicate a negative moment (the raft rotated towards North) in the upper part, turning into positive moments below +3 m a.s.l.. The numerical model predicts higher absolute values both for the positive and negative moments.

These differences may be attribuited to several causes: the most important one may be the occurrence of viscous strains in the fresh concrete. An evaluation of the effects of this phenomenon is not carried out up to now but in the next future, further calibration tests will be planned to investigate this aspect.

Finally, it is interesting to note that the strains produced but the application of the load in the acceptance tests are in accordance with the design prediction, that is the load formed by 6 trucks on the bridge induced a vertical deformation in the upper part of pile around 9 με compatible with the pile stiffness measured during the load test described by Bersan et al. This confirms the effectiveness of the monitoring system installed in the pile.

7 REFERENCES

Bersan S., Bergamo O., Palmieri L., Schenato L., Simonini P. (2018). Distributed strain measurements in a CFA pile using high spatial resolution fibre optic sensors. Engineering Structures 160, 554–565.

Brownjohn J. M.W. (2007). Structural health monitoring of civil infrastructure. Philosophical Transactions of the Royal Society A, 365, 589-622.

Cunat, P. (2012). Detection and evaluation of leaks through embankment hydraulic structures, by distributed temperature analysis, measured by fiber optics, Ph.D. thesis, University of Grenoble, Grenoble, France.

De Battista N, Kechavarzi C, Seo H, Soga K, Pennington S. (2016) Distributed fibre optic sensors for measuring strain and temperature
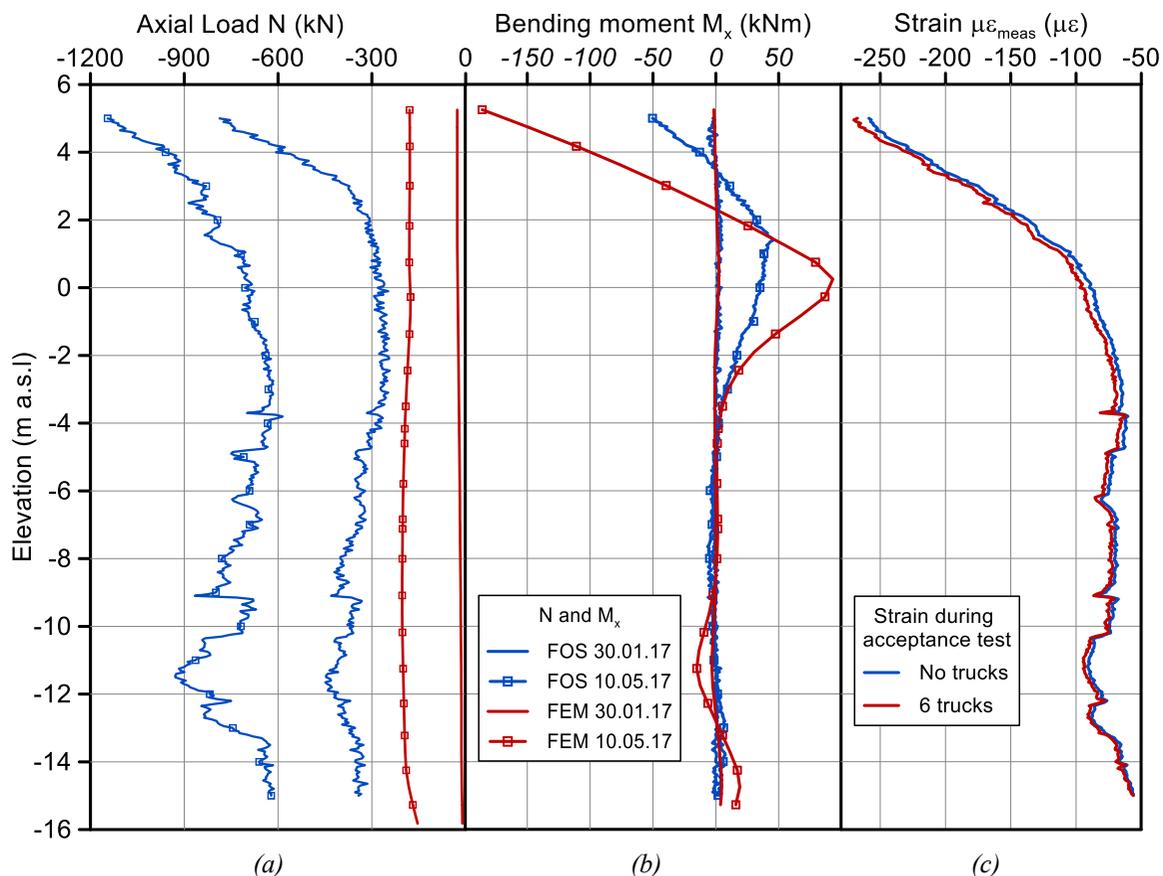
Figura 4. (a) Measured and simulated axial forces at steps (b) and (d); (b) Measured and simulated bending moments respect X local axisat steps (b) and (d); (c) $\mu\varepsilon_{meas}$ recorded by the DFOSs on 30.01.2017 during the acceptance test in condition without and with 6 trucks on the bridge.

of cast-in-situ concrete test piles. In: IC on smart infrastructure and construction (ICSIC), Cambridge, UK, 27–29 June 2016. ICE Virtual Library.

Kania, J. and Sorensen, K.K. (2018) A static pile load test on a bored pile instrumented with Distributed Fibre Optic Sensors. 10th International Symposium on Field Measurements in Geomechanics, Rio de Janeiro. In printing.

Palmieri L., Schenato L. (2013). Distributed Optical Fiber Fensing Based on Rayleigh Scattering. The Open Optics Journal, 7, (Suppl-1, M7) 104-127.

Schenato L. (2017). A review of distributed fibre optic sensors for geo-hydrological applications. Appl. Sci., 7, 1-42.

Schenato L., Palmieri L., Camporese M., Bersan S., Cola S., Pasuto A., Galtarossa A., Salandin P., Simonini P. (2017). Distributed optical fibre sensing for early detection of shallow landslides triggering, Scientific Reports. DOI:10.1038/s41598-017-12610-1.

Soga K. (2014). Understanding the real performance of geotechnical structures using an innovative fibre optic distributed strain measurement technology. Rivista Italiana di Geotecnica, 4, 7-47.